

# A method for estimating 2D wrinkle ridge strain from application of fault displacement scaling to the Yakima folds, Washington

Daniel Mège

Laboratoire de Tectonique, Université Pierre et Marie Curie, Paris, France

Stephen P. Reidel<sup>1</sup>

Pacific Northwest National Laboratory, Richland, Washington

**Abstract.** The Yakima folds on the central Columbia Plateau are a succession of thrust anticlines thought to be analogs of planetary wrinkle ridges. They provide a unique opportunity to understand wrinkle ridge structure. Field data and length-displacement scaling are used to demonstrate a method for estimating two-dimensional horizontal contractional strain at wrinkle ridges. Strain is given as a function of ridge length, and depends on other parameters that can be inferred from the Yakima folds and fault population displacement studies. Because ridge length can be readily obtained from orbital imagery, the method can be applied to any wrinkle ridge population, and helps constrain quantitative tectonic models on other planets.

## Introduction

This study is motivated by inference from other planetary bodies (Mercury, Venus, Mars, Moon) that wrinkle ridges, as defined by *Watters* [1993], are probably the most widespread contractional structures in the inner Solar System [e.g., *Watters*, 1988], and the conclusion that developing a method for estimating strain at wrinkle ridges is necessary to constrain any quantified tectonic model for these bodies. To this end, strain distribution needs to be calculated in two dimensions (2D) at least, if not three. The Yakima folds (also called Yakima ridges) on the Columbia Plateau are the best wrinkle ridge analogs on Earth, as discussed by *Watters* [1988] and *Mège and Ernst* [2001], and provide a unique opportunity to determine a wrinkle ridge structure model from which two-dimensional strain (map view) can be obtained. In another method, *Watters et al.* [1998] used maximum displacement-length scaling to infer maximum contractional strain at Mercurian lobate scarps, which are structures in part similar to wrinkle ridges [*Schultz*, 2000]. However their method does not consider displacement variations along faults, and therefore gives 1D strain only.

## Yakima Folds

The Yakima ridges (Figure 1) are a dozen anticlinal ridges [e.g., *Reidel et al.*, 1994] whose structural style calls for a

combination of broad-scale folding and thrusting displaying great complexity [*Tolan and Reidel*, 1989] and cutting across the whole Columbia River Basalt Group (CRBG) volcanic pile [*Lutter*, 1994]. Despite the uncertainties due to the outcropping conditions, several ridges are known in great detail (references in *Reidel et al.*, [1994]). Major thrusts extend along the ridges [*Reidel et al.*, 1994] conferring systematic asymmetric ridge profile [*Reidel et al.*, 1994], and suggesting that folding is closely related to faulting. Fault-bend folding and fault-propagation folding are both consistent with field observations *Price and Watkinson* [1989]. Although these kinematic models may be only rough approximations of actual deformation [*Schultz*, 2000], they certainly provide a good insight into the bulk deformation mechanism. Here we assume that these models are accurate enough to provide reliable approximations of Yakima ridge deformation given the uncertainty of other parameters used to calculate strain. A fundamental consequence of these models is that shortening along the Yakima ridge thrust planes is a measure of total ridge shortening.

## Method

The method we use is based on maximum displacement-length scaling of faults and published displacement profiles along terrestrial fault end zones. Displacement and length data at the Yakima ridges reported in this paper have been obtained from geological and geophysical investigations. They provide important constraints for further fault scaling studies as only few displacement-length data at thrust faults have been published.

Mean ridge length at the Yakima fold belt is on the order of 100 km (Table 1). Most ridges, however, are composed of segments having variable length. Linkage of two fault segments is strong if segment separation  $2s$ , overlapping  $2o$ , and spacing between fault mid-points  $2k$  are such that  $s/k < 0.2$  and  $o/k > -0.5$ , where the minus sign expresses underlap [*Schultz*, 1999]. Following this criterion, most fault segments at the Yakima ridges identified by *Tolan and Reidel* [1989] are strongly linked [*Mège and Reidel*, 2000], suggesting that mechanically, the fault segments behave as if they were replaced by a single fault having length  $L$ , the total ridge length, and maximum displacement  $d_{max}$ , the displacement that would be expected from scaling laws for single segments [*Dawers and Anders*, 1995]. Usual displacement-length scaling can reasonably be applied to the Yakima ridges on the basis of one ridge - one fault of similar length. In 2D, maxi-

<sup>1</sup>Also at Washington State University, Pullman

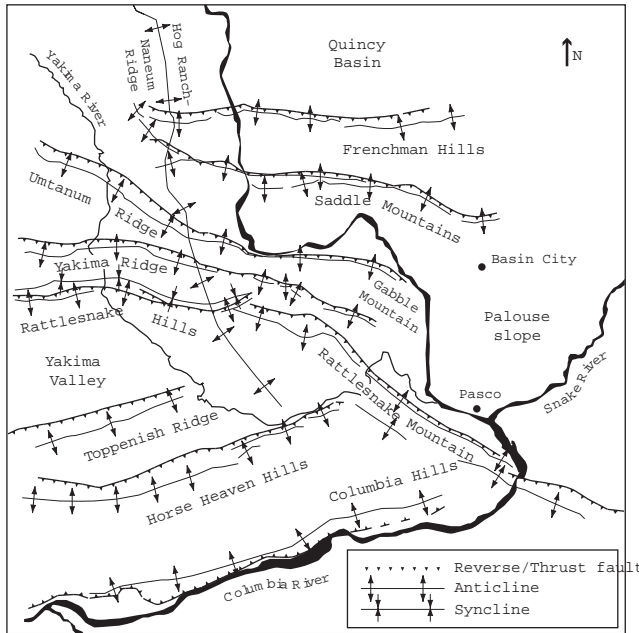


**Figure 1.** Simplified structure map of the Yakima folds, central Columbia Plateau. A detailed map can be found in *Tolan and Reidel* [1989].

imum displacement-length scaling is of the form [e.g., *Cowie and Scholz*, 1992a, *Schlische et al.*, 1996]

$$\gamma = d_{max}/L \quad (1)$$

where  $\gamma$  is a measure of critical shear strain for fault propagation. This simple relation has been derived from single structures as well as complex fault zones [*Dawers and Anders*, 1995]. It has been shown to apply to normal and strike-slip faults as well as thrust faults [*Elliott*, 1976; *Cowie and Scholz*, 1992a; *Dawers and Anders*, 1995], and does not depend on fault size [*Dawers et al.*, 1993]. Although  $\gamma$  values are well documented over several orders of fault length [*Cowie and Scholz*, 1992a], the plausible range of  $\gamma$  for a given length spans over two orders of magnitude due to uncertainty induced by 2D approximation in displacement-length scaling modeling [*Schultz and Fossen*, 2000]. Therefore the scaling law is not predictive in its current formulation, and the best estimates to date for determining  $\gamma$  at a given fault set still come from observation. Displacement data from geological and geophysical observations at the Yakima ridges will help determine a reliable  $\gamma$  value using eq. (1).

At a first approximation, Linear Elastic Fracture Mechanics predicts an elliptic fault plane along with displacement (Figure 2a) that also exhibits an elliptic profile [e.g., *Cowie and Scholz*, 1992b] giving the horizontal shortened surface area  $A_{el}$  as

$$A_{el} = (\pi/4)d_{max}L \cos \alpha \quad (2)$$

where  $d_{max}$  is observed at fault center, and  $\alpha$  is mean fault dip angle. However, inelastic (plastic) fault tip propagation frequently results in tapered or linear fault displacement profile [*Cowie and Scholz*, 1992a, 1992b], usually linear [*Cowie and Shipton*, 1998]. The elastic solution (eq. 2) therefore overestimates the shortened surface area. We propose that a good approximation of the shortened surface

**Table 1.** Yakima ridge data

Ridge	$L, km$	$d_{Hmax}, km$	$\alpha, ^\circ$
Umtanum Ridge	110	1-3	28-45
Rattlesnake Mtn + rattles	100	3-6	19-35
Manastash Ridge	55	3-6	9-17
Saddle Mountains	110	3-6	19-33
Horse Heaven Hills	185	2-4	24-42
Rattlesnake H.-Ahtanum R.	85	1-2	22-36
Yakima Ridge	100	3-6	23-40
Frenchman Hills	100	0.3-2	18-34
Toppenish Ridge	85	1-2	14-27
Columbia Hills	170	2-4	10-20
Cleman Mountain	35	1-2	21-36
Snipes Mountain	110	0.5-1	21-36
Bezley Hills	160	1-2	21-36
Badger Hills	50	1-2	21-36
mean	104	1.6-1.4	21-36
standard deviation	44	1.0-1.9	10-13

The data have been compiled from previous works, most of them cited in the text. Length  $L$  has been obtained from field observations and geologic mapping. Strike variation along fault trace length due to topographic effect was removed. Maximum horizontal displacement  $d_{Hmax} = d_{max} \cos \alpha$  was retrieved from field observations. For each of the first 10 ridges on Table 1, mean fault dip angle  $\alpha$  was inferred from combination of field measurements and available seismic profiles. The mean dip angle from these ridges was used as  $\alpha$  values for the 4 remaining ridges where no data are available.

area is provided by the sum of three coalescing geometric features. An elliptical surface area  $A_1$  between the inner boundary of both fault end zones, of length  $L - 2s$  where  $s$  is the length of a fault end zone, accounts for elastic displacement profile at the fault center. Two wedges  $A_2/2$  of length  $s$  at both fault tips abutting on ellipse  $A_1$  account for linear displacement decrease toward fault ends (Figure 2b).

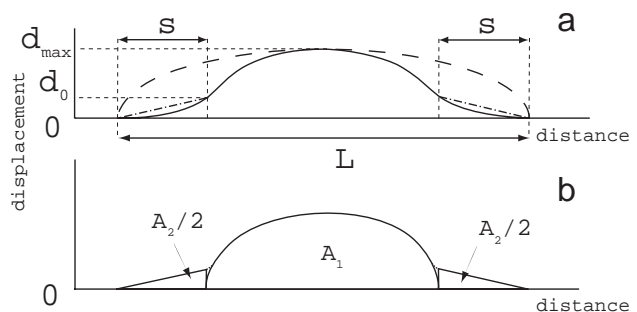


**Figure 2.** (a) Elastic fault displacement profile (dashed line) and mixed elastic-inelastic fault displacement profiles. Solid line: extrapolation of Dugdale crack to shear fractures predicting tapered fault ends (after *Cowie and Scholz* [1992b]); dashed-dotted line: updated profile predicting linear fault tip profile (after *Cowie and Shipton* [1998]). (b) Geometry of shortened surface area as modeled in this paper. The dashed line highlights the difference between this model and the model that would result from the theoretically linear fault tip displacement profile.

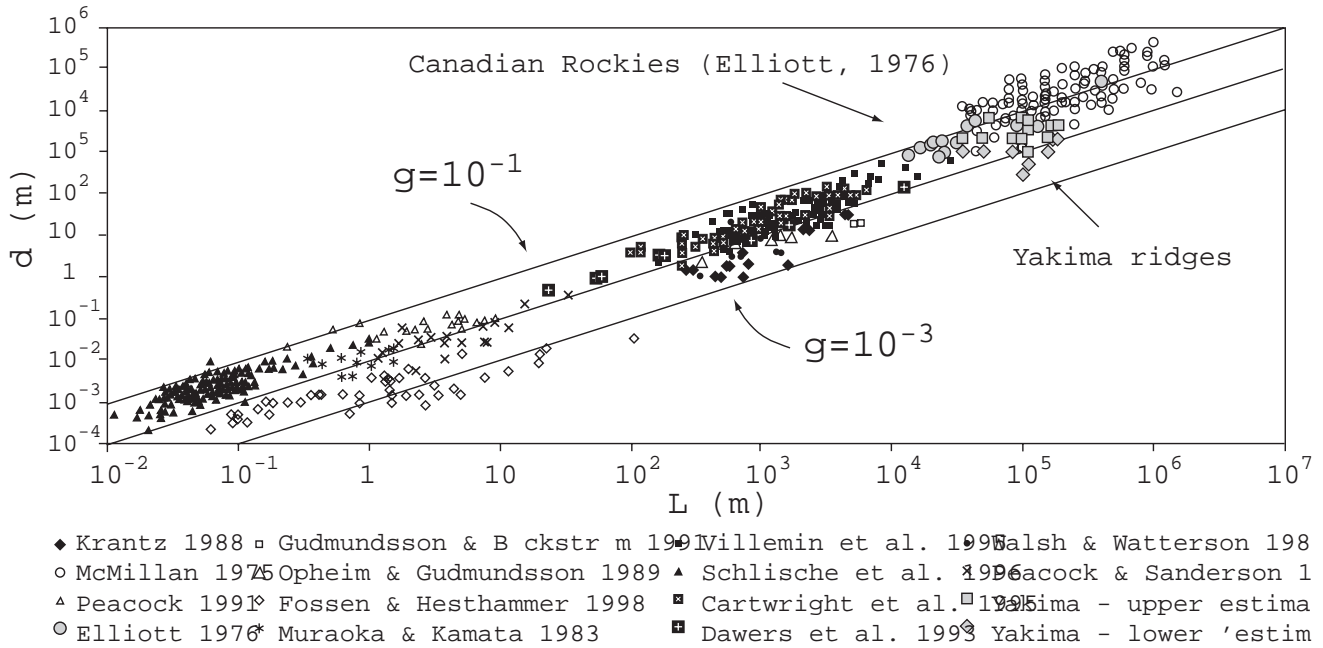


**Figure 3.**  $d - L$  plot for Yakima ridges and other shear fracture data sets (fault sets referenced in *Schlische et al.* [1996], and deformation bands from *Fossen and Hesthammer* [1998]). Error bars for the Yakima ridges are provided by uncertainty on maximum displacement.

The total shortened area is given by

$$A_{el+in} = A_1 + A_2 = [(\pi/4)(L - 2s)d_{max} + sd_0] \cos \alpha \quad (3)$$

where  $d_0$  is displacement at distance  $s$  from the fault tip. Analysis of available data sets suggests that a linear relation exists between  $d_{max}$  and  $d_0$ . *Cowie and Scholz* [1992b] use 0.35 and 0.18 as a preferred value for  $d_0/d_{max}$  and  $s/L$ , respectively. By taking more recent data sets into account we find 0.26 (standard deviation 0.16) and 0.16 (standard deviation 0.08), respectively [*Mège and Reidel*, 2000]. For application to wrinkle ridges, where maximum displacement is unknown,  $d_{max}$  may be replaced by  $\gamma$  in eq. (1). By combining eq. 1 and 3

$$A_{el+in} = [(\pi/4)(L - 2s)\gamma L + sd_0] \cos \alpha \quad (4)$$

Shortening calculated using eq. (3) or (4) is ca. 70 % lower than shortening using elastic theory (eq. 2) alone.

## Results from the Yakima folds

Shortening is calculated from the data in Table 1 using both the elastic model (eq. 2) and the elastic-inelastic model (eq. 3). The structural and geophysical investigations carried out to date at the Yakima ridges do not yet allow to infer accurate along-strike displacement variations at fault ends. For this reason we have no observational means to favor one model or the other. From earlier studies, the elastic model is thought to be appropriate for decreasing fault propagation rate whereas the elastic-inelastic model is thought to approximate faults having constant propagation rate [*Peacock*, 1996]. *Reidel* [1984] showed that dramatic Saddle Mountains growth occurred in a few hundred thousand years at most while most of the CRBG erupted between 17 and 15.5 Ma, then it almost stopped although minor deformation is still ongoing. Thus, the displacement rate has been highly

variable from 17 Ma on, but approximately constant from 15.5 Ma on, which suggests that typical fault end zone displacement profile at the Yakima ridges may be intermediate between elliptic and linear.

Shortening calculated using eq.(2) and (3) is in the range 1148-3754 km<sup>2</sup>, depending on uncertainty in  $d_{max}$  and  $a$ . Given the 163,700 km<sup>2</sup> Columbia Plateau surface area [*Tolan et al.*, 1989], plateau strain is found to be 0.7 - 2.3%. Contractional strain at the Yakima Fold subprovince [e.g., *Reidel et al.*, 1994], which is about half the total Columbia Plateau surface area, is therefore found to be within the range 1.4 - 4.6%. These values are 2 to 10 times smaller than previous 1D shortening estimates of 10-15 % along a given N-S profile across the Yakima ridges [*Reidel et al.*, 1989]. This difference is due to the fact that calculation of 2D strain accounts for strain variations along fault, whereas calculation of 1D strain accounts for strain across a single profile. Extrapolation of 1D strain to 2D would require that strain measured at one site along a fault is representative of displacement along the entire fault, which is not correct as displacement must decrease toward fault tips. Since 1D strain is usually calculated where displacement is supposed to be maximum, extrapolation to 2D significantly overestimates real 2D strain.

The kinematic models of fold growth we assumed do not explicitly include strain along backthrusts, which are quite commonly observed at the Yakima ridges (as well as at wrinkle ridges [*Schultz*, 2000]). However, backthrust displacement relieves displacement that would have occurred on the main thrust [*Niño et al.*, 1998; *Schultz*, 2000], so that backthrusts and associated folds are implicitly included in the analysis above. Since we accounted for all the Yakima ridges and for fault segment linkage, strain at minor faults, which may be significant [*Scholz*, 2000], is expected to be in great part accounted for as well. Thus, the

calculated strain may be lower than, but probably close to total Yakima ridge strain. Minor additional strain would be obtained by considering the transverse Hog Ranch-Naneum ridge [Reidel *et al.*, 1989], but it is not related to the Yakima folds and therefore its study is out of the scope of this paper.

### Application to planetary wrinkle ridges

A displacement-length plot (Figure 3), from Yakima ridge data in Table 1 and other terrestrial shear fracture data sets, confirms theoretical prediction that the Yakima ridges fit the linear scaling law in eq.(1) and provides  $\gamma$  estimates that may be extrapolated to planetary wrinkle ridges. Mean  $\gamma$  is found to lie between  $1.9 \times 10^{-2}$  and  $3.9 \times 10^{-2}$ .

Assuming a realistic fault dip angle for wrinkle ridges, such as provided by the mean Yakima fault dip angle reported on Table 1 (which is typical of thrust fault dip angles), calculating strain only requires measuring ridge length on images or maps and application of eq.(4) or combination of eqs. (1) and (2). If wrinkle ridge deformation involves the whole elastic lithosphere, then wrinkle ridge strain obtained using our method has direct implications for its thickness when the ridges formed, and helps constrain heat flow evolution through time.

### References

- Cowie, P. A., and Scholz, C. H., Displacement-length scaling relationship for faults: data synthesis and discussion, *J. Struct. Geol.*, *14*, 1149-1156, 1992a.
- Cowie, P. A., and Scholz, C. H., Physical explanation for the displacement-length relationship of faults using a post-yield fracture mechanics model, *J. Struct. Geol.*, *14*, 1133-1148, 1992b.
- Cowie, P. A., and Shipton, Z., K., Fault tip displacement gradient and process zone dimensions, *J. Struct. Geol.*, *20*, 983-997, 1998.
- Dawers, N. H., and Anders, M. H., Displacement-length scaling and fault linkage, *J. Struct. Geol.*, *17*, 607-614, 1995.
- Dawers, N. H., Anders, M. H., and Scholz, C. H., Growth of normal faults: Displacement-length scaling, *Geology*, *21*, 1107-1110, 1993.
- Elliott, D., The energy balance and deformation mechanisms of thrust belts, *Phil. Trans. R. Soc. London*, *283*, 289-312, 1976.
- Lutter, W. J., Catchings, R. D., and Jarchow, C. M., An image of the Columbia Plateau from inversion of high-resolution seismic data, *Geophysics* *59*, 1278-1289, 1994.
- Mège, D., and Ernst, R. E., Contractional effects of plumes on Earth, Venus, and Mars, in *Locating pre-Mesozoic mantle plumes*, edited by R. E. Ernst and K. L. Buchan, K. L., Geol. Soc. Am. Sp. Pap., 352, 2001 (in press).
- Mège, D., and Reidel, S. P., Two-dimensional strain at wrinkle ridges using fault-displacement length scaling at terrestrial analogs (abstract), *Abstr. Progr.* *32* (7), Geol. Soc. Am. Ann. Meet., 2000.
- Niño, F., Philip, H., and Chry, J., The role of bed-parallel slip in the formation of blind thrust faults, *J. Struct. Geol.*, *20*, 503-416, 1998.
- Peacock, D. C. P., and Sanderson, D. J., Effects of propagation rate on displacement variations along faults, *J. Struct. Geol.*, *18*, 311-320, 1996.
- Price, E. H., and Watkinson, A. J., Structural geometry and strain distribution within eastern Umtanum fold ridge, south-central Washington, in *Volcanism and tectonism in the Columbia River flood-basalt province*, edited by S. P. Reidel and P. R. Hooper, Geol.Soc. Am. Sp. Pap., 239, 265-281, 1989.
- Reidel, S. P., The Saddle mountains: the evolution of an anticline in the Yakima fold belt, *Am. J. Sci.*, *284*, 942-978, 1984.
- Reidel, S. P., Fecht, K. R., Hagood, M. C., and Tolan, T. L., The geologic evolution of the central Columbia Plateau, in *Volcanism and tectonism in the Columbia River flood-basalt province*, edited by S. P. Reidel and P. R. Hooper, Geol.Soc. Am. Sp. Pap., 239, 247-264, 1989.
- Reidel, S. P., Campbell, N. P., Fecht, K. R., and Lindsey, K. A., Late Cenozoic structure and stratigraphy of South-Central Washington, *Washington Div. Geol. Earth Res. Bull.*, *80*, 159-180, 1994.
- Schlische, R. W., Young, S. S., Ackermann, R. V., and Gupta, A., Geometry and scaling relations of a population of very small rift-related normal faults, *Geology*, *24*, 683-686, 1996.
- Scholz, C. H., and Cowie, P. A., Determination of total strain from faulting using slip measurements, *Nature*, *346*, 837-839, 1999.
- Schultz, R.A., Fault-population statistics at the Valles Marineris extensional province, Mars: Implications for segment linkage, crustal strains, and its geodynamical development, *Tectonophysics*, *316*, 169-193, 1999.
- Schultz, R. A., Localization of bedding-plane slip and backthrust faults above blind thrust faults: Keys to wrinkle ridge structure, *J. Geophys. Res.*, *105*, 12,035-12,052, 2000.
- Schultz, R. A., and Fossen, H., Displacement-length scaling in three dimensions: the importance of aspect ratio and application to deformation bands (abstract), *Eos Trans. AGU*, *81*(48), Fall Meet. Suppl., F1185, 2000.
- Tolan, T. L., and Reidel, S. P., Structure map of a portion of the Columbia River flood-basalt province, scale 1:500,000, in *Volcanism and tectonism in the Columbia River flood-basalt province*, edited by S. P. Reidel and P. R. Hooper, Geol. Soc. Am. Sp. Pap., 239, Map, 1989.
- Tolan, T. L., Reidel, S. P., Beeson, M. H., Anderson, J. L., Fecht, K. R., and Swanson, D. A., Revisions to the estimates of the areal extent and volume of the Columbia River Basalt Group, in *Volcanism and tectonism in the Columbia River flood-basalt province*, edited by S. P. Reidel and P. R. Hooper, Geol. Soc. Am. Sp. Pap., 239, 1-20, 1989.
- Watters, T. R., Wrinkle ridge assemblages on the terrestrial planets, *J. Geophys. Res.*, *93*, 10236-10254, 1988.
- Watters, T.R., Compressional tectonism on Mars, *J. Geophys. Res.*, *98*, 17049-17060, 1993.
- Watters, T.R., Robinson, M. S., and Cook, A. C., Topography of lobate scarps on Mercury: new constraints on the planet's contraction. *Geology*, *26*, 991-994, 1998.

D. Mège, Laboratoire de Tectonique, Boite 129, Université Pierre et Marie Curie, 75252 Paris cedex 05, France. (e-mail: dmege@lgs.jussieu.fr)

S. P. Reidel, Pacific Northwest National Laboratory, PO Box 999, Richland, WA 99352. (e-mail sp.reidel@pnl.gov)

(Received January 31, 2001; revised April 2, 2001; accepted May 07, 2001.)